Astron. Astrophys. 167, 341–350 (1986)

ASTRONOMY AND ASTROPHYSICS

Very small particles in spiral galaxies

S.K. Ghosh[1,2], **S. Drapatz**[1], **and U.C. Peppel**[1]

[1] Max-Planck-Institut für extraterrestrische Physik, D-8046 Garching bei München, Federal Republic of Germany
[2] Tata Institute of Fundamental Research, Homi Bhabha Road, Bombay-400005, India

Received May 12, accepted June 30, 1986

Summary. The existence of a hot component of very small dust particles in normal spiral galaxies has been inferred from a statistical study of their infrared emission as measured by IRAS. Our galaxy has been demonstrated to be a typical spiral and is used to investigate various emission sources for mid-infrared radiation. Young and evolved discrete objects are shown to be of minor importance. Rather, evidence is presented for the diffuse nature of the mid-infrared radiation of galaxies. A fairly quantitative treatment of the emission process leads to the observed quantities.

Key words: interstellar dust – spiral galaxies – mid-infrared emission – H II regions – IRAS

1. Introduction

Normal spiral galaxies constitute a major fraction ($\sim 35\,\%$) of all galaxies. In infrared wavelengths ($5\,\mu m \leqq \lambda \leqq 200\,\mu m$) they are on an average much more luminous than the ellipticals and lenticulars. This is primarily due to the fact that spirals have relatively more interstellar matter, ISM ($\sim 10\,\%$ by mass), i.e. more interstellar dust, which converts the short wavelength emission of heating sources into infrared radiation. Hence the large scale galactic infrared emission is ideally suited to study the interaction of the stars and the ISM in a spiral galaxy.

The main hurdle to these studies have been the poor sensitivity of detectors and strong interference of the earth's atmosphere in the mid-infrared, MIR, ($\lambda \sim 10\,\mu m$) and far-infrared, FIR, ($\lambda \sim 100\,\mu m$) wavelengths which results in lack of observations of a large sample of spiral galaxies although there have been several attempts using balloon and air borne telescopes.

With the advent of the Infrared Astronomy Satellite (IRAS), the situation has changed dramatically. In the *IRAS Point Source Catalog*, about 10,000 known galaxies and about a similar number of "galaxy-like" objects have been detected at one or more of the four photometric bands of the IRAS Sky Survey experiment (Neugebauer et al., 1984). Based on the preliminary results of the brighter galaxies, about $\sim 65\,\%$ of all the galaxies detected are expected to be normal spirals. Although most of these galaxies have been detected only at 60 μm and/or 100 μm bands, still there is a significant number (several hundreds) of them having measured fluxes in all the four IRAS bands.

Send offprint requests to: S. Drapatz

On the basis of the new data it is now possible for the first time to investigate the emission properties of spirals in the whole mid-infrared to far-infrared spectrum using a statistically significant sample. As known from our own galaxy, specifically the nature of the mid-infrared radiation is poorly understood. Showing our galaxy to be a typical example of normal spirals regarding its infrared emission properties, one can conclude that the underlying physical mechanisms responsible for the observed quantities in the majority of spirals are the same. Hence our galaxy and the sample of spirals are studied simultaneously.

The mid-infrared radiation has to originate from a hot dust component, which is expected in the close environment of H II regions. Keeping this in mind, a statistical comparison has been made between a sample of spiral galaxies and another of galactic H II regions in Sect. 2. This shows that the dust associated with the H II regions is not the hottest component and is not the major contributor to the MIR emission of spirals. Therefore in Sect. 3, other possible sources of MIR emission (some of which have been discussed in the literature) are considered in the light of the IRAS measurements. This investigation follows in three parts dealing with the emission by young objects, evolved objects and by very small particles in the general interstellar medium.

Section 4 summarizes the present work and the conclusion that the existence of very small particles is a common feature of normal spirals and that they are the major source of MIR emission on the galactic scale.

2. Comparison of galaxies and H II regions

2.1. Data

The measurements used in the present study originate from the IRAS sky survey experiment. The unbiased all sky survey has been performed at four broad photometric bands with centre wavelengths 12, 25, 60, and 100 μm. In the following, the first band is refered to as MIR and the other three bands together as FIR. Detailed descriptions are available in the Explanatory Supplement (ES, Beichman et al., 1985).

Two standard products of the IRAS mission which have been used extensively here are: the IRAS Point Source Catalog (hereafter IPSC) and the Low Resolution All Sky Images (hereafter LORASI). The former lists all the confirmed point like sources (approximate definition of "point" source: FWHM $\leqq 0\farcm8$ at 12 and 25 μm, $\leqq 1\farcm5$ at 60 μm, and $\leqq 3'$ at 100 μm) with their

measured photometric fluxes (or upper limits) in the four bands. The latter provides the flux densities in $\frac{1}{2}^\circ \times \frac{1}{2}^\circ$ pixels for almost the complete sky in all the four bands for each of the three separate "hours confirmed" sky coverages (known as HCONs; see ES).

2.2. *Sample S of galaxies and Sample H of* H II *regions*

As the hotter dust component is responsible for MIR emission, it was thought that a comparison of the infrared spectral shapes of the spiral galaxies with that of the galactic radio H II regions in a statistical manner may provide important information about the MIR emission on a galactic scale. One should get a good indication about what fraction of the luminosity of all O stars ($5\ 10^9\ L_\odot$, including evolved H II regions) is converted into MIR.

The sample of galaxies has been generated, for operational simplicity, by using all the galaxies of ESO/Uppsala Catalogue (Lauberts, 1982) detected at all the four bands by IRAS (IPSC) and having their classification as "normal galaxy" in the ESO catalogue. As the IRAS detection criteria itself predominantly selects the spirals, (see IRAS minisurvey results, Soifer et al., 1984), the estimated non-spiral contamination does not affect the present analysis. Also, demanding detections in all four IRAS bands does not bias the sample towards the galaxies with stronger MIR emission. The validity of the last two remarks is shown in Sect. 2.3. Our sample contains 215 galaxies and is referred to as Sample S.

Galactic radio H II regions are mainly found in the galactic plane and are best identified by their free-free radio continuum emission at decimetric wavelengths. At present the most complete radio continuum surveys of the galactic plane at ~ 6 cm (5 GHz) wavelength are the Bonn (Altenhoff et al., 1979) and the Parkes (Haynes et al., 1979) surveys. Hence the sample of galactic H II regions was generated by taking all the IPSC sources identified with any of the above two survey sources. A sample of 328 galactic H II regions (Sample H) was found with measured fluxes in all the four IRAS bands. It becomes clear in Sect. 2.3 that, demanding all four band detections does not bias the sample towards the H II regions with stronger MIR emission as no H II regions with relatively stronger 12 μm emission have been found in the sample.

In Appendix A we show that the sample sources are smaller than the IRAS beams, and hence the IPSC fluxes are meaningful for our study.

2.3. *Comparison*

To quantify the infrared spectral shapes of different class of objects, two dimensionless parameters α and γ have been defined where the former is a measure of the ratio of FIR to MIR emission and the latter quantifies the spectral shape of FIR emission. These parameters can be readily calculated from the measured fluxes in the four bands as given below:

$$\alpha = \log_{10}\left(\frac{P_{25}+P_{60}+P_{100}}{P_{12}}\right), \tag{1}$$

$$\gamma = \log_{10}\left(\frac{P_{60}+P_{100}}{P_{25}}\right). \tag{2}$$

Here, P_λ is the power received in the λ micron band given by

$$P_\lambda = S_\nu \cdot (\Delta\nu)_\lambda, \tag{3}$$

where S_ν is the flux density (Jansky) listed in the IPSC and $(\Delta\nu)_\lambda$ is an instrumental factor resembling the effective bandwidth (Hz). Using the relative system responses in the four bands (see ES, Table II. C. 5), and keeping in mind that the quoted IPSC flux densities refer to an assumed source spectrum of the type $S_\nu \sim \nu^{-1}$ within the photometric band (ES, Section VI. C. 3), one obtains $(\Delta\nu)_{12} = 1.35\ 10^{13}$ Hz, $(\Delta\nu)_{25} = 5.15\ 10^{12}$ Hz, $(\Delta\nu)_{60} = 2.57\ 10^{12}$ Hz, and $(\Delta\nu)_{100} = 9.95\ 10^{11}$ Hz.

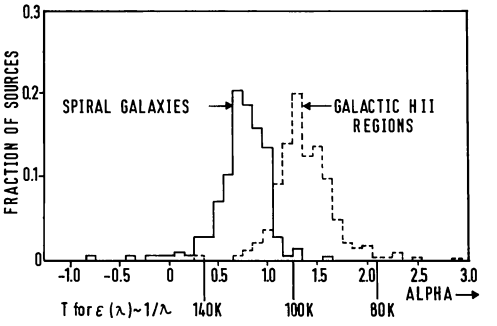

Fig. 1. The distributions of α, which is a measure of FIR to MIR emission ratio, for the samples of spiral galaxies (215) and the galactic H II regions (328) are presented. Schematic dust temperatures corresponding to α, for an emissivity law $\varepsilon_\lambda \sim \lambda^{-1}$ are shown

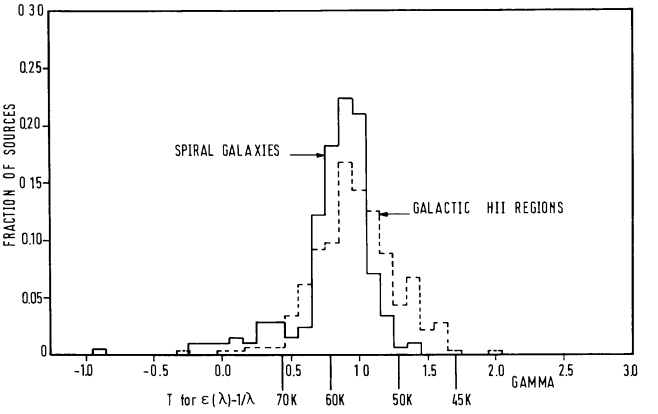

Fig. 2. The distributions of γ for the samples of spiral galaxies (215) and the galactic H II regions (328) are presented. Schematic dust temperatures corresponding to γ, for an emissivity law $\varepsilon_\lambda \sim \lambda^{-1}$ are shown

The distribution of the parameters α and γ in the samples of spiral galaxies (S) and the galactic H II regions (H) are presented in Figs. 1 and 2 respectively. The heavy line refers to the sample S and the dashed one to the sample H. The distributions are normalized such that the areas under them are equal.

From both distributions, values indicative of dust temperatures T(K) have been obtained, assuming a dust emissivity law $\varepsilon_\lambda \sim \lambda^{-1}$ in the entire wavebands of IRAS. The values are marked below the abscissas in the figures. While the dust temperatures corresponding to γ roughly represent physically meaningful quantities for emission of dust particles in thermal equilibrium, the numbers obtained from α are unrealistically high, especially for the galaxy sample. As discussed later, the temperature has no direct physical meaning, since non-equilibrium processes are involved.

Two things are immediately evident from Fig. 1: (i) For both the samples, there is a tight constraint on the range of the parameter α as is clear from the half-widths of the distributions. They correspond to the narrow ranges in the (FIR/MIR) ratio of ~ 2.8 for the spiral galaxies and ~ 3.4 for the galactic H II regions. The near universality of the parameter α within a given sample, further strengthens our conclusion (see Appendix A) that these

sources are not spatially extended compared to the IRAS beams in respective bands and the IPSC fluxes are not underestimates. The narrow range of α also demonstrates the fact that the galaxy sample is not biased favourably towards the galaxies with stronger MIR emission, as in that case one would expect an extension of the α distribution towards the smaller values. (ii) The mean of the distribution for Sample H is distinctly shifted to the higher values of α compared to the Sample S. This shift corresponds to a factor ~ 5 increase in the ratio of FIR to MIR emission.

If, (i) the contemporary ideas about the origin of the galactic FIR emission (e.g. de Muizon and Rouan, 1985; Cox et al., 1986) are correct and (ii) our Galaxy is a typical spiral galaxy regarding its FIR and MIR emission (in fact this point will be demonstrated in Sect. 3.3), then the above statistical comparison leads one to conclude that the dust associated within and nearby H II regions is not hot enough to be the major contributor of MIR emission of spiral galaxies in general. The O stars outside H II regions, which contribute about 80 % of all ionizing stars, correspond to an even larger value of $\alpha \sim 3$ (see Fig. 7 of Cox et al., 1986). Thus it is clear that this conclusion is valid for all the ionizing stars.

The situation is, however, different for the parameter γ, which is sensitive to the spectral shape between 25 μm and 100 μm. This parameter has similar values for the radio H II regions, extended H II regions, the galactic plane as well as spiral galaxies in general. Identical distributions are already obtained for these samples if one considers the range between 60 and 100 μm only (power ratios).

Another parameter for investigation of FIR is the infrared excess, IRE, defined as $L_{IR}/N_c' h\nu_{Ly\alpha}$. It ranges between 3 and 7 (Puget, 1985; Mezger, 1985) for ionizing stars and has a value of ~ 12 for the inner part of our Galaxy (Caux et al., 1984) with a trend to reduce with the galactocentric distance (Caux et al., 1985). Since the possible contribution of ionizing stars to FIR can be estimated from the ratio of IRE of the stars to that of the galaxy, a substantial fraction (~ 50 %) of the FIR emission (in the IRAS bands) in spiral galaxies originates from the ionizing regions.

This is consistent with the observed similarity of γ distributions of H II regions and spirals, as well as with the fact that the contribution of radio H II regions (obtained by adding up IPSC intensities), which contain ~ 20 % of all ionizing stars, is about 10 % of the total galactic FIR emission as measured by IRAS.

3. Sources of MIR emission

In order to identify alternative sources of MIR emission in spiral galaxies in general, we firstly show that our galaxy is a representative spiral regarding its total mid- and far-infrared emission properties. Next, the contributions to the MIR luminosity from various types of prospective sources have been assessed for this typical spiral galaxy.

3.1. The total MIR and FIR emission

Using LORASI the galactic emission and its longitude distribution at the four IRAS bands have been determined. A preliminary analysis of the IRAS data has already shown (Hauser et al., 1984) that the zodiacal emission (ZE) tremendously dominates the galactic emission (GE) at 12 and 25 μm throughout the galactic plane and is still comparable to the GE at 60 and 100 μm in outer parts of the galactic plane. Also instrumental effects are important. Therefore, a careful evaluation of the ZE contribution is necessary and has been discussed in Appendix B.

The resulting galactic and zodiacal emission in all the four IRAS bands are presented in Fig. 3. They display the galactic longitude distributions of the brightness in the 12, 25, 60, and 100 μm bands respectively. The solid and the dashed lines refer to the GE and ZE respectively. At 12 and 25 μm the ZE is larger than the scale of the figure, near the ecliptic plane crossings. The longitude distributions of GE clearly show the stronger emission from the Galactic centre and the 5 kpc arm region in all the four IRAS bands.

Using the above results, an average value for the FIR/MIR ratio, α (and also γ) for our Galaxy has been computed by treating each galactic longitude bin independently and weighting them according to their intensity contribution. In the 12 μm and 25 μm bands simple correction factors of the type $\tau/(1-e^{-\tau})$ for the self-absorbing dusty medium have been estimated, where the optical depth τ has been obtained like in Cox et al. (1986), but τ has been averaged over the observed latitude range (FWHM of the emissivity $\sim 3°$). One gets similar correction factors ~ 1.3 in both the bands and the resulting values are: $\alpha_{gal} = 0.63$ (or $\langle \text{FIR/MIR} \rangle_{gal} = 4.3$) and $\gamma_{gal} = 0.88$. The average values of α and γ for the Galaxy falls at the peak of the distributions of α and γ for the sample of spiral galaxies (see Figs. 1 and 2). This shows that our Galaxy is a typical spiral galaxy as far as its FIR and MIR emission is concerned.

To obtain an estimate of the absolute MIR luminosity, the average brightness of the most luminous part of the Galactic plane in and around MIR, has been plotted in Fig. 4. The averaging in galactic longitude and latitude are according to the availability of observations (except for LORASI, see below). The average brightness in all four IRAS bands have been computed from LORASI by making appropriate corrections for the zodiacal emission (see Appendix B). The average brightness corresponding to Little and Price (1985) has been computed from their quoted values of peak galactic ridge emission and their latitude distribution halfwidths. The averaging has been effected such that their values can be directly compared with those of LORASI ones. The agreement between them is remarkable. The higher values corresponding to Price (1981) are easily understandable as they have been averaged only over $|b| \leqq 1°$. Expected error in the brightness values in MIR is at most a factor of ~ 2.

The total galactic MIR luminosity can be estimated from Fig. 4, by modelling the spatial distribution of the emitting regions in the Galaxy and correcting for the extinction. A very crude assumption that most of the MIR luminosity ($8\,\mu\text{m} \leqq \lambda \leqq 15\,\mu\text{m}$) originates from the 5 kpc ring leads to a value $\sim 10^9\, L_\odot$ which is a rather conservative lower estimate.

3.2. The contributions of young objects

In Sect. 2.3 it has been noticed that the H II regions are not the major source of MIR ($\lambda \sim 10$ μm) emission for spiral galaxies. This has been found to be true for our Galaxy as well. Recently de Muizon and Rouan (1985) have modelled the mid and far infrared emission in the Galaxy by considering the dust emission of diffuse H I clouds, dense molecular (H_2) clouds, H II regions associated with OB clusters and the regions of active star formation. A comparison of their computed spectrum with observations immediately shows that although the FIR part of the spectrum is very well explained by their model, none of the four components considered can explain the observed MIR emission of the Galaxy.

In what follows, other possible sources of MIR emission in the galaxy have been considered, specifically using IRAS data. Candidates with FIR/MIR $\geqq 10$ (like H II regions, see Sect. 2.3) must be rejected as they would have already been recognized as the

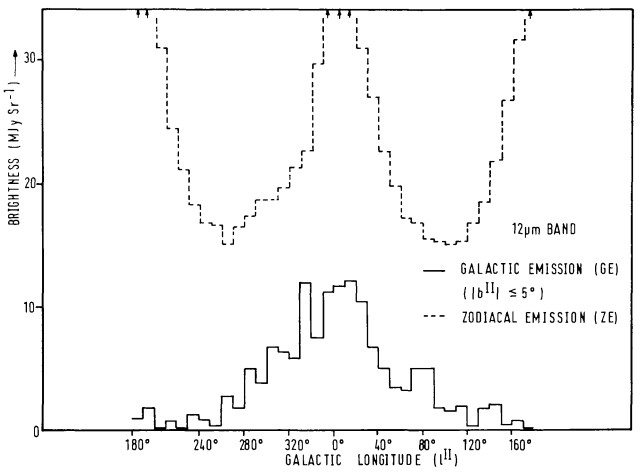

Fig. 3a. The galactic longitude distribution of the 12 μm emission from the galactic plane as computed from the IRAS Low Resolution All Sky Images

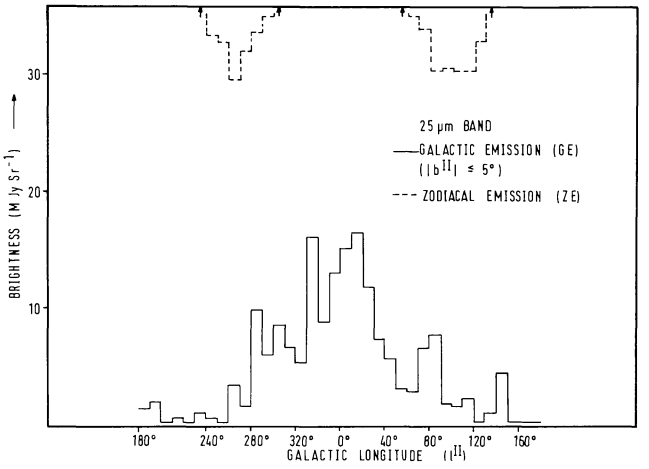

Fig. 3b. The galactic longitude distribution of the 25 μm emission from the galactic plane as computed from the IRAS Low Resolution All Sky Images

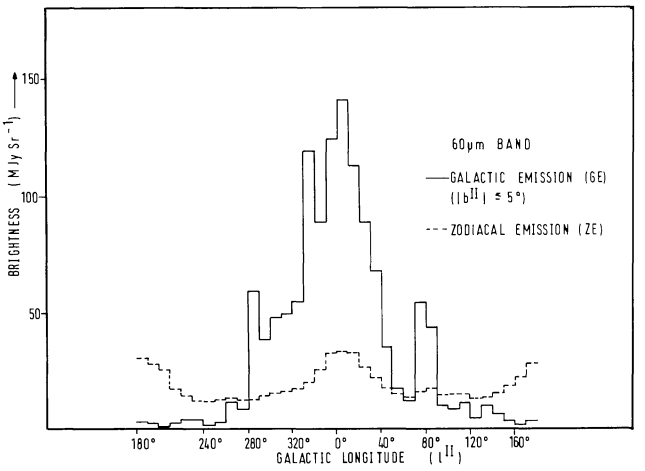

Fig. 3c. The galactic longitude distribution of the 60 μm emission from the galactic plane as computed from the IRAS Low Resolution All Sky Images

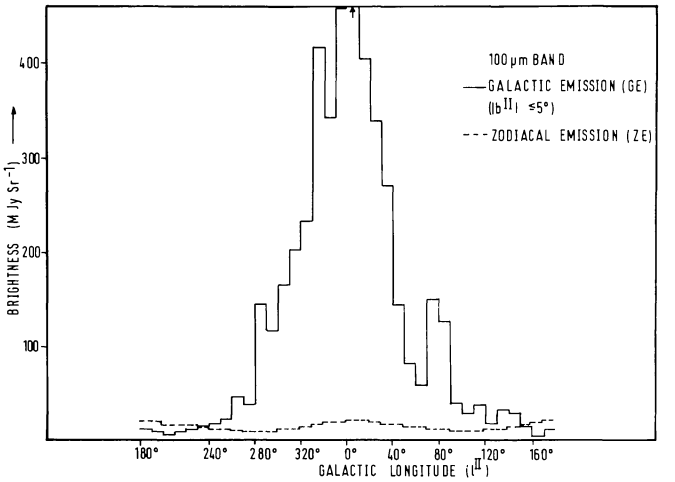

Fig. 3d. The galactic longitude distribution of the 100 μm emission from the galactic plane as computed from the IRAS Low Resolution All Sky Images

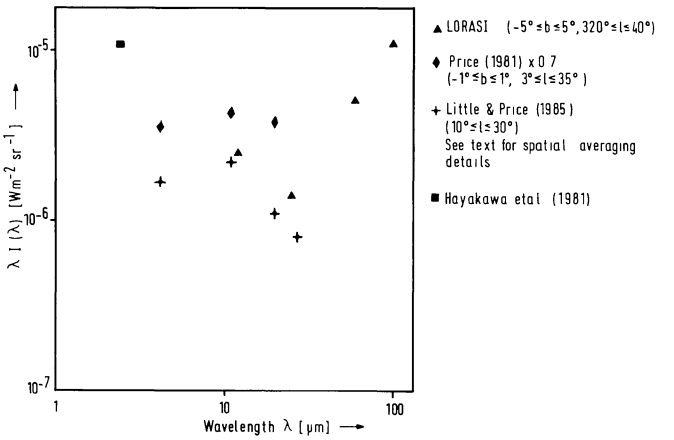

Fig. 4. The observed spectra of infrared emission from some selected regions of the inner galactic plane

most prominent galactic FIR source. This argument rules out globules completely and protostars partially (see measurements of Keene et al., 1980, 1982).

A total contribution of star forming regions in the Galaxy can be very generally estimated from the available gravitational energy and making the assumption that the ratio of mass to radius is fairly constant during various phases of the collapse. For a star formation rate (SFR) $\sim 10\, M_\odot\, \mathrm{yr}^{-1}$ and the universal initial mass function, this value is $10^8\, L_\odot$. But even, a much stricter upper limit to the contribution of young objects to the galactic MIR luminosity can be obtained by discussing different types of objects in detail. This will be presented in the following.

A recent calculation by Adams and Shu (1985) show that for protostars in mass accretion stage with core mass $\sim 1\, M_\odot$, the ratio FIR/MIR $\geqq 10$. However, while comparing their calculations with observations of three well studied objects (B 335, IRS 1-B 5 and L 1551-IRS 5) representing a sequence of increasing age, an enormous excess in the MIR is noticed for the second and the third object. Interestingly enough IRS 1-B 5, the young protostellar

source has its observed FIR to MIR ratio (Beichman et al., 1984), about unity! IRS 1-B 5 is believed to be a protostar (age $\leqq 10^5$ years) leading to $\sim 1\,M_\odot$ ZAMS star (Benson et al., 1984, Beichman et al., 1984) and has its total luminosity $\sim 10\,L_\odot$, with $\sim 1\,L_\odot$ in $\lambda \geqq 100\,\mu$m and $\sim 3\,L_\odot$ at $\lambda \leqq 12\,\mu$m. This makes the protostars in the stage of evolution similar to IRS 1-B 5 attractive candidates for galactic MIR emission, although the emission mechanism/(s) are still unclear.

An estimate of the contribution to the galactic MIR emission from "IRS 1-B 5-like-protostars" can be made using the mass and MIR luminosity of IRS 1-B 5, the observed Galactic star formation rate, a universal initial mass function and the duration (τ) of such objects in "IRS 1-B 5-like" phase. Using a total SFR in the Galaxy as before, one obtains the total MIR luminosity due to such objects in the galaxy to be

$$L_{\text{Protostars}}(\text{MIR}) \sim 10^7 \left(\frac{\tau\,(\text{yr})}{10^5}\right) L_\odot \sim 10^{-2}\, L_{\text{Galaxy}}(\text{MIR}). \qquad (4)$$

As τ is not expected to be much larger than 10^5 years (Benson et al., 1984; Lada, 1985), these sources fall short of the galactic MIR emission by two orders of magnitude.

Next we consider the class of objects resembling the source L 1551-IRS 5 which has a ratio FIR/MIR ~ 4 (Emerson et al., 1984). This source is associated with energetic molecular outflow (EMO). According to the present belief (Lada, 1985), all protostars go through the stage of EMO in their evolution towards main sequence.

In a recent review, Lada (1985) has listed 68 outflow sources documented to date. Certainly many observational and geometrical biases intrinsic to the sources go into the identification of these sources. Still, a crude order of magnitude estimate of their number in the Galaxy can be made. Of the 68 sources listed, 55 have estimated distance $d \leqq 1$ kpc and 34 of them $d \leqq 0.5$ kpc. This shows that the efficiency of detection (say, η) of these EMO's is far from unity even in the local neighbourhood. Making the crude assumption of their uniform distribution in the Galactic disk and using the above numbers, one expects $\sim (10^4/\eta)$ sources in the Galaxy. Their contribution to the galactic MIR luminosity is

$$L_{\text{EMO}}(\text{MIR}) \sim \left(\frac{5\ 10^4}{\eta}\right) L_\odot = \left(\frac{5\ 10^{-5}}{\eta}\right) L_{\text{Galaxy}}(\text{MIR}) \qquad (5)$$

assuming L 1551-IRS 5 to be a typical EMO source (MIR luminosity $\sim 5\,L_\odot$). One needs $\eta \leqq 10^{-4}$ to explain the galactic MIR emission from these sources alone. Although our assumption of uniform distribution of sources throughout the Galaxy (especially in the 5 kpc arm) and the use of the solar neighbourhood source density are gross underestimates, still a value of $\eta \sim 10^{-4}$ (remember, it refers to the detection efficiency for sources within 0.5 kpc only) cannot be reconciled with.

T-Tauri stars (TTS) are pre-main sequence stars of mass $\sim 0.5 - 2\,M_\odot$, contracting towards the main sequence. They have a near infrared emission continuum which extends up to mid-infrared and beyond. From a recent statistical study of a sample of T-Tauri stars in the Taurus molecular cloud complex, Harris (1985) has shown that the ratio of their average far infrared to the mid infrared luminosity is only ~ 1.5.

The total expected number of TTS in the Galaxy is calculated using the number of known radio H II regions (i.e. $\sim 20\,\%$ of all O stars), assuming an universal initial mass function, assuming the average mass of TTS $\sim 1\,M_\odot$ and that of stars giving rise to H II regions $\sim 15\,M_\odot$. If $\tau_{\text{H II}} \sim 5\ 10^5$ yr (Mezger, 1978) and $\tau_{\text{TTS}} \sim 10^5$ yr (Lada, 1985) are the average lifetimes of H II regions and the T-Tauri phase of evolution, then the total TTS contribution to the galactic MIR luminosity is

$$L_{\text{TTS}}(\text{MIR}) \sim 10^7 \left(\frac{\tau_{\text{TTS}}}{\tau_{\text{H II}}}\right) f^{-1}\, L_\odot \leqq 10^{-2}\, L_{\text{Gal}}\,(\text{MIR}), \qquad (6)$$

where $f \sim 0.1 - 0.5$ is the fraction of all galactic H II regions detected in the radio continuum surveys as a result of source confusion and finite detection threshold.

Recently, two types of sources have been explored (Puget et al., 1985, Cox et al., 1986) to explain the galactic MIR emission. They are (*i*) hot ($\sim 300°$ K) circumstellar dust shells of high massloss stars (e.g. OH/IR stars) and (*ii*) very small grains (radius $\geqq 5$ Å) heated by the general interstellar radiation field. In the next paragraph we consider the plausibility of the above sources for explaining the MIR emission of spiral galaxies in general.

3.3. *The contribution of evolved objects*

The circumstellar dust shells of high massloss stars have temperatures high enough ($T \sim 200 - 500$ K) to emit mostly in 5 to 20 μm region. These shells have sufficient optical thickness to convert a major fraction of the central stellar luminosity into MIR. Objects, which might contribute a significant fraction of the galactic MIR luminosity have to be numerous enough and need sufficiently long lifetime in the mass loss phase. Corresponding stars (with a few solar masses) have ages of $\sim 10^8$ years, whereas the FIR emission of the spiral galaxies is dominated by young and massive stars (O or B) during their main sequence lifetime $\sim 5\ 10^6$ years. As a result, if the evolved stars were mainly responsible for the MIR emission of spiral galaxies, then the ratio FIR/MIR would be sensitive to the past star formation rate if the SFR has not been constant over time scales of the order of $\geqq 10^8$ years. To look for this effect, a test has been made using a sample of galaxies with evidence for time dependent SFR, namely star burst galaxies and interacting or merging galaxies.

The star formation rate in the interacting/merging galaxies as a class is supposed to have been augmented by star formation bursts triggered by interactions. The estimated increase in SFR from near and mid infrared observations has been found to be ~ 3 (Lonsdale et al., 1984). The efficiency of galaxy-galaxy interactions for inducing starbursts is almost 100 % (Joseph et al., 1984).

Presently, a sample of interacting galaxies has been generated for studying their FIR/MIR or α distribution. This sample is a subset of all the galaxies in the Morphological Catalogue of Galaxies (MCG, Vorontsov-Velyaminov and Krasnogorskaja, 1962; Vorontsov-Velyaminov and Arhipova, 1964, 1963, 1968, 1974) which are classified as "interacting" and listed in the appendices of the MCG. There are a total of 1852 interacting systems listed in the MCG. As MCG is complete up to ~ 15 mag (Sandage, 1975) in the region of the sky covered by it, it is expected to be a fairly homogeneous sample of interacting galaxies. Of these, 717 have been detected by the IRAS survey experiment and are listed in the IPSC. However, as for studying the α distribution, measured fluxes at all the four IRAS bands are required, we were left with 86 of them. Hereafter, this sample is referred to as Sample I. The α distribution of Sample I is shown in Fig. 5. The distribution is identical to that for the normal (non-interacting) spirals' Sample S (see Fig. 1). This displays the insensitivity of the ratio FIR/MIR to the history and the absolute value of the star formation rate.

In addition, a comparison of absolute luminosities in the IRAS bands for two samples of (i) normal and (ii) interacting/starburst galaxies, for which a distance estimate is available, have been

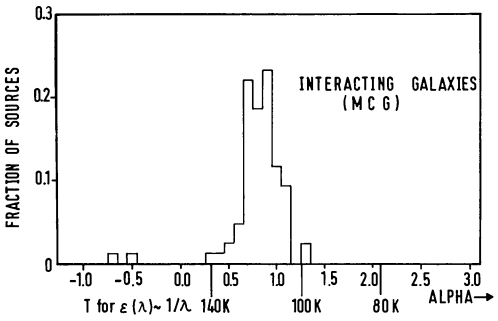

Fig. 5. The distribution of α, which is a measure of FIR to MIR emission ratio, for the sample of interacting galaxies (86). Schematic dust temperatures corresponding to α, for an emissivity law $\varepsilon_\lambda \sim \lambda^{-1}$ are shown

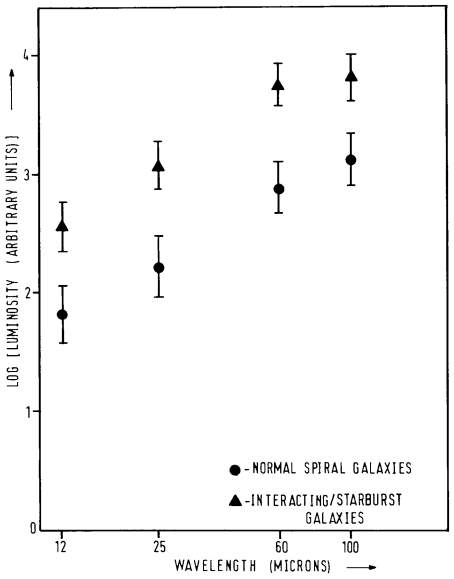

Fig. 6. The average IRAS band luminosities of two samples of normal (20) and interacting (15) spiral galaxies with distance estimates, are plotted. The 1σ error on the mean is shown

made. The normal galaxy sample consists of NGC galaxies and the interacting ones are from the Arp Catalogue (Arp, 1966). The average luminosities of the two samples in the four IRAS bands are plotted in Fig. 6 for comparison. Although the statistics is not ideal (sample size $\sim$15–20), still it demonstrates the fact that on an average, the increase in FIR luminosity of interacting galaxies is also accompanied by an almost identical increase in MIR luminosity so as to keep the FIR/MIR ratio same as that for the normal galaxies.

From the above discussion, it is evident that the sources of energy for MIR emission in spiral galaxies are time correlated with those of FIR emission. This is in conflict with the picture that the evolved stars are responsible for a major fraction of the MIR luminosity in spirals, if starbursts do not last $\geqq 10^8$ years.

Next, we consider the contribution of evolved stars to the galactic MIR emission in the light of IRAS point source catalogue. One prominent example is OH/IR stars. These stars are post main sequence stars at almost the end of their stellar evolution. Their progenitor mass is in the range 2–5 $M_\odot$ (Herman and Habing, 1985) and the OH/IR phase is relatively short lived ($\sim 10^4 - 10^5$ years) as compared to their main sequence lifetime ($\geqq 10^8$ years).

As the luminosity of the OH/IR stars is $\sim 10^3 - 10^4\, L_\odot$, almost all OH/IR stars in the Galaxy will have detectable fluxes ($\sim$1 Jy) at 12 μm band of IRAS (Olnon et al., 1984). Of course, source confusion may hinder their detection in the regions of high source density close to the galactic centre. In a region $\sim 25°$ away from the galactic centre (but in the galactic plane), the completeness of the IPSC at 12 μm, for sources with flux densities above 1 Jy is $\geqq 63\,\%$ for regions with two HCON coverages and $\geqq 88\,\%$ for regions with three HCON coverages (see Section VIII. D. 5 of ES). Still, to be on the safer side, we have considered the galactic longitude region $90° \leqq l^{II} \leqq 100°$ where the IPSC completeness should be much better than the above numbers.

An absolute upper limit on the OH/IR stars' contribution to the observed brightness at 12 μm, in the longitude bin $90° \leqq l^{II} \leqq 100°$, can be obtained by adding the fluxes of *all point sources* in IPSC having 12 μm detection and lying in that longitude bin. This point source contribution to the 12 μm brightness is smaller than the total galactic emission (as computed from the LORASI) by a factor $\sim$15. Hence it is clear that the contribution of the OH/IR stars to the MIR brightness of the Galaxy in the region $l^{II} \sim 95°$ is insignificant. By considering other longitude bins further than $\sim 40°$ from the galactic centre, it has been checked that the above conclusion is insensitive to the particular choice of the longitude bin where the comparison of the contribution of discrete sources is made with the total emission. In fact, the fractional contribution of the discrete sources at 12 μm decreases further as one approaches the galactic centre. Although, this could partially be due to the source confusion effects, these effects can certainly not be very large, since a concentration of OH/IR stars in the 5 kpc ring, obtained from earlier results (Herman and Habing, 1986), is a factor $\sim$4 higher. But this by itself is an upper limit in the new light of the galactic longitude distribution of spectrally selected IRAS point sources. If the relative contribution of all types of objects are similar between $l^{II} \sim 90°$ to $\sim 30°$, then again an upper limit of a factor $\sim$4 is obtained from Fig. 3 (a).

In addition, to strengthen our above conclusion, a statistical test has been made to look for source confusion effects in the IPSC sources in the longitude bin $90° \leqq l^{II} \leqq 100°$. The distribution of the number of IPSC sources dN (in this longitude bin) with their flux densities in the range $S_{12\,\mu m}$ and $S_{12\,\mu m} + dS_{12\,\mu m}$ (or in other words the differential source counts), have been studied as a function of $S_{12\,\mu m}$ (Jy). The resulting distribution is shown in the form of $\log |(dN/d\log S_{12})|$ *vs.* $\log S_{12}$ in Fig. 7. The effect of source confusion is to flatten the slope of this curve at flux densities lower than the value at which the source confusion sets in. Figure 7 shows no evidence for flattening up to a flux density $\sim$0.25 Jy which itself is below the completeness level of IPSC at 12 μm ($\sim$0.4 Jy, Rowan-Robinson et al., 1984). The above statistical test performed on the sample of IPSC sources in the neighbouring longitude bins also gives identical results.

Actually, the above result applies not only to OH/IR stars, but also to all discrete sources detected by IRAS. If the distribution of stellar populations in the Galaxy is similar to that in the solar neighbourhood, their total contribution can be estimated by extrapolating the $\log N - \log S_{12\,\mu m}$ curve (see Fig. 7) of IRAS detected sources. To explain the total galactic 12 μm brightness by these point sources, the amount of extrapolation needed correspond to unrealistically large distances ($\sim$10 times the galactic size) for reasonable MIR luminosity of these stars.

3.4. *Emission of very small particles*

The last paragraphs have shown that the MIR emission of the galaxy originates not from point-like sources, but is of diffuse interstellar origin. This is best explained by a component of very

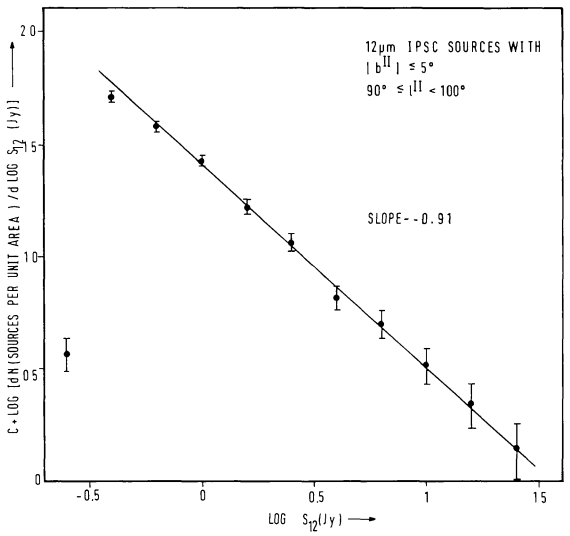

Fig. 7. The differential source counts of all the IRAS point source catalog sources detected at 12 μm and lying in the region $90° \leqq l^{II} \leqq 100°$, $|b^{II}| \leqq 5°$ are shown. It shows no evidence for flattening down to a flux density of ~0.4 Jy

small particles in the galactic dust. Following the suggestion by Léger and Puget (1984) and Puget et al. (1985) we assume that these particles are single polycyclic aromatic hydrocarbon chain molecules with sizes between 4 and 15 Å containing less than 300 carbon atoms. Their lattice modes are excited by the absorption of a single UV photon leading to a transient heating to about 1000 K and subsequent MIR emission in bands between 3 and 15 μm. It is assumed that this process determines the emission in the 12 μm IRAS band, while the far-infrared radiation in the three other IRAS bands is due to emission of the normal grain (Mathis et al., 1977) component, where the grains have well defined temperatures for the sizes ≧100 Å (Drapatz and Michel, 1977). Then the parameter α characterizes the ratio between the contributions of these two dust components. This parameter will be derived in the following for our galaxy.

Since the excitation of the small particles is mostly due to UV photons, we consider two components of the interstellar radiation field: photons below the Balmer discontinuity (uv) and above it (vis). Using the local interstellar radiation field u (multiplied by the speed of light) and the absorption optical depth τ (Drapatz, 1979), the total far-infrared emission of the normal dust component is given by

$$\varepsilon^{\odot}(\mathrm{FIR}) = \langle\tau(\mathrm{vis})\rangle\,\langle u(\mathrm{vis})\rangle + \langle\tau_n(\mathrm{uv})\rangle\,\langle u(\mathrm{uv})\rangle$$
$$= 1.6\ 10^{-22}\,\langle u(\mathrm{vis})\rangle + 4.7\ 10^{-22}\,\langle u(\mathrm{uv})\rangle\,. \quad (7)$$

Here, $\langle\tau\rangle$ and $\langle u\rangle$ are wavelength averaged quantities. The total mid-infrared emissivity is estimated using the absorption efficiencies and particle size distribution for the small particles as described by Puget et al. (1985). Then,

$$\varepsilon^{\odot}(\mathrm{MIR}) = \langle\tau_s(\mathrm{uv})\rangle\,\langle u(\mathrm{uv})\rangle = 2\ 10^{-21}\,f(C)\,\langle u(\mathrm{uv})\rangle\,. \quad (8)$$

The optical depth τ_s is a function of $f(\mathrm{C})$, the fraction of all carbon atoms locked up in small particles. As long as $f(\mathrm{C}) \leqq 0.1$ one has $\tau_n \geqq \tau_s$, i.e. the normal dust component controls the radiative transport in the interstellar UV radiation field. If the small particles are two-dimensional, the projection effect will decrease τ_s by a factor up to 2.

The solar neighbourhood values $\varepsilon^{\odot}$ have been converted to the corresponding average galactic values ε^{G} using the scaling factors given in the paper by Drapatz (1979), then

$$\frac{\varepsilon^{G}(\mathrm{FIR})}{\varepsilon^{G}(\mathrm{MIR})} = \frac{0.23\,\langle u(\mathrm{uv})\rangle + 0.07\,\langle u(\mathrm{vis})\rangle}{f(\mathrm{C})\,\langle u(\mathrm{uv})\rangle}\,. \quad (9)$$

Knowing the spectral distribution of the mid-infrared (Léger and Puget, 1984) as well as the far-infrared (Pajot et al., 1986) emissivity, one can derive the intrinsic α, which is based on observations in the IRAS bands

$$\alpha = \log\left(\frac{1}{f(\mathrm{C})}\left(0.1\,\frac{\langle u(\mathrm{vis})\rangle}{\langle u(\mathrm{uv})\rangle} + 0.3\right)\right). \quad (10)$$

The parameter α depends on $f(\mathrm{C})$, and on the ratio R of the long wavelength to the short wavelength interstellar radiation fields. For our galaxy, R is approximately 2 yielding $f(\mathrm{C}) \sim 0.1$ for the observed $\alpha = 0.63$ and

$$\alpha \simeq \log(3 + R)\,. \quad (11)$$

Similar values of α (in the range 0.7–1.0) have been observed in central regions of reflection nebulae (e.g. NGC 7023, NGC 2071 IR), whose central stars are of type B 3 with R ratios similar to the average galactic radiation field.

Since the fractional far-infrared power in the IRAS bands is fairly constant for all spiral galaxies (see γ distribution in Fig. 2), Eq (11) applies to other galaxies as well.

Even if the UV radiation field is increased drastically, (small R in Eq 11), the parameter α does not change significantly for the same dust population, i.e. it is not surprising that all other spiral galaxies and even interacting/merging spirals have a similar α (see Figs. 1 and 5). This has also been shown for individual galaxies. More detailed mid-infrared observations of M 31 (by IRAS) and M 82 (Gillett et al., 1975; Willner et al., 1977) have been interpreted (Walterbos and Schwering, 1985; Désert et al., 1986) as the emission of small particles, where M 82 spectra actually show the emission of at least two molecular bands characterizing the emitters.

As seen from Eq (10), the parameter α is sensitive to two effects: (i) strong relative increase of the long wavelength radiation field and (ii) change in the amount of carbon atoms locked up in small particles. An example for the first case can be found in elliptical galaxies, where there actually exist indications for $\alpha \geqq 1.0$. However, corresponding observations are only starting to become available (Impey et al., 1986). The second case occurs in small regions, where very high UV radiation fields evaporate the smallest grains and thereby reduce $f(\mathrm{C})$. One observes $\alpha = 1.2$–1.7 for regions close to O stars (see e.g. α distribution for H II regions in Fig. 1) and for the central regions of reflection nebulae with B 1/B 2 stars (e.g. NGC 2023, NGC 2071 H II). The increase of α i.e. the decrease of the mid-infrared radiation field by a factor of 5, can be made plausible by mentioning that out to a distance of 1 pc of an O star, small particles ≦10 Å are evaporated (Puget et al., 1985). This results in a reduction of the emission by a factor of 4 as compared to the interstellar population of small particles.

The picture of very small particles is also consistent with the observed insensitivity of the $\langle\mathrm{FIR/MIR}\rangle$ ratio to the possible non-universal initial mass function (IMF) in the star-burst galaxies (Rieke et al., 1980; Kronberg et al., 1985).

Hence, from our statistical analysis of the sample of spiral galaxies, we conclude that very small particles are a common feature in these galaxies as evident from their MIR emission.

4. Conclusions

Our Galaxy has been demonstrated to be a very typical spiral as far as its mid- and far-infrared emission is concerned. Therefore, it has been studied further to explore various possible sources of the mid-infrared emission of galaxies.

Young objects like H II regions, protostars, energetic molecular outflow sources and T-Tauri stars have been considered in detail using IRAS observations. Specifically, a statistical comparison of the mid- and far-infrared emission of a sample of spiral galaxies and galactic H II regions has shown that the dust associated with the H II regions is not the hottest component and can not be the major contributor to the mid-infrared emission of spiral galaxies in general. Also the other discrete young objects turn out not to be responsible for MIR emission of spirals.

The possible contribution of evolved objects has also been discussed using the recent IRAS measurements (Point Source Catalog and the All Sky Images). It has been shown, that the estimated cumulative contribution of all discrete sources as obtained by extrapolating the log N-log S (differential source counts) curve of discrete sources, in directions relatively free from source confusion effects, is much smaller than the observed (diffuse + discrete) emission. Statistical evidences have been presented which show that the ratio of far- to mid-infrared emission is independent of present and past star formation rate by further comparing the samples of interacting and starburst galaxies. The stellar evolution time scale arguments contradict the hypothesis that the circumstellar dust shells of evolved stars are the major source of mid-infrared emission on the galactic scale. This implies that evolved discrete objects are also not the main contributors to MIR emission.

The most natural explanation for the origin of the MIR emission of spiral galaxies is small particles heated transiently by individual energetic photons of the interstellar radiation field. Their emission traces, though with lower contrast than FIR emission, the star formation activity of galaxies. One might take advantage of the possible higher spatial resolution in this wavelength band to study extragalactic objects. Using the ideas of Puget et al. (1985) for the very small particles, we derive a relation between the FIR/MIR emission ratio, the fraction of carbon atoms locked up in these particles, and the UV and visible radiation fields. On the basis of this interpretation the FIR/MIR ratio of H II regions, spiral galaxies and even interacting galaxies can be understood fairly quantitatively.

Acknowledgements. It is a pleasure to thank Dr. Andrew Strong for his help in computer access to the IRAS All Sky Maps and Drs. A. Léger and J.L. Puget for the useful discussions. One of us (S.K.G.) thanks the Max-Planck-Institute for the warm hospitality.

Appendix A

Effects of finite source size and IRAS beams

One of the several criteria for including any possible detection into the IPSC is that its scan profile closely resembles the "point source template" of the corresponding waveband. This has been quantified (for details see ES) by a parameter "Point Source Correlation Coefficient" (CC). The numerical value of CC is sensitive to the source extension along the scan direction and the local signal to noise ratio. While source candidates with CC $\geqq 0.87$ (and $\geqq 0.97$ for high source density regions), have been considered for inclusion in IPSC, all sources of our samples H and S have CC $\geqq 0.98$.

For both the samples H and S it was investigated, what fraction may possibly be extended relative to the IRAS beams using the information about the data processing for the Small Extended Source Catalog. This catalog contains sources with angular sizes between $\sim 3'$ and $8'$. In the IPSC, the number of small extended sources in the given band in a $6'$ (in-scan) $\times 4'.5$ (cross-scan) area centered on each source, are listed ("SES 2", see ES for details).

It has been found that at least 50% of the sources in sample S and H, have SES 2 = 0 in all four bands, meaning that they are not extended and also their fluxes are not contaminated by nearby extended objects. The distribution of the flux dependent parameters used in the present study (α and γ, see Sect. 2.3), for these sub-samples are identical to the same for the respective complete samples. This demonstrates the fact that the IPSC fluxes for the sources in our samples S and H are very good measures of their total emission.

The above test has also been performed for the sample of interacting galaxies (described in Sect. 3.2) with identical conclusions.

Other independent observational results have been used to justify that most of our sample sources are point-like for IRAS beams. First we consider sample H.

A number of galactic H II regions have been mapped in the mid and far infrared in detail, with comparatively smaller beams, from balloon borne and air borne telescopes. From these studies, one gets an idea about the physical extents of MIR and FIR emitting regions of H II regions in general.

High resolution maps of Frogel and Persson (1974) at 10 μm and of Frogel et al. (1977) at 10 and 20 μm lead to average angular sizes (FWHP) $\leqq 30''$ for distances larger than a few kpc. A part of the galactic plane has been surveyed at ~ 70 μm with a $1'$ beam by Jaffe et al. (1982) and Stier et al. (1982). Average angular size of this sample of H II regions is $\bar{\theta}_{70\,\mu m} \sim 1'.4 \pm 0'.9$. Incidentally, about 20 of these H II regions appear in the 5 GHz survey catalogue of Altenhoff et al. (1979) which has been used in selecting Sample H for the present study.

Although the above mentioned observations are sensitive to the brightness gradients (using beam chopping on the sky), their angular size measurements are reliable as the chopper throws were larger than the estimated angular sizes in the respective wavebands.

From the above discussion, it is clear that for most of the sources belonging to the sample of H II regions (Sample H), the source sizes in the MIR and FIR are smaller than the IRAS beams in the respective bands. Only very nearby H II regions have no proper representation in our sample. However, checks of these individual sources do not show any different infrared characteristics.

The sample of spiral galaxies (Sample S) has been selected from the ESO/Uppsala catalogue, which lists the major (and minor) axis diameters of each galaxy. This optical (blue) size roughly refers to (Lauberts, 1982) a level slightly below 25 mag/square arc second. As most of the blue emission originates from the early type stars, its spatial distribution in spiral galaxies is closely coupled to that of their far infrared emission. Also, for a random distribution of inclinations "i", the blue sizes of most of the galaxies are expected to be unaffected by extinction. The distribution of the major axis diameters of all the galaxies in this catalogue show a peak at $\sim 1'.15$ (see Table 3 of Lauberts, 1982). This is also roughly the median value of the distribution. The Sample S, which is a subset of the ESO/Uppsala catalogue, also shows a similar distribution.

A realistic FWHM of the brightness distribution of these galaxies has been obtained using the above average major axis diameter and 15 mag. as the average total integrated magnitude.

The most probable optical size of these galaxies is equal to (i) $\sim 0'.4$ for an exponential fall outwards in the galactic plane and (ii) $\sim 0'.8$ for a corresponding Gaussian model. In either case, their sizes are smaller than or at most comparable to the IRAS beams in all the four bands.

Finally, a direct test has been made to look for the size dependence of the IRAS observed infrared spectral properties (relevant to the present study) for the galaxy Sample S. The complete Sample S has been sub-divided into smaller but statistically significant subsets according to their optical sizes (major axis diameters quoted in ESO/Uppsala catalogue). The distribution of the observed physical parameters used in the present study are identical for these subsets, thereby demonstrating their size independence and consolidating our earlier remarks.

Appendix B

Estimation of zodiacal emission in LORASI

The brightness of the ecliptic plane depends on the solar elongation angle "*El*" of the IRAS telescope boresight, during the measurements. This brightness change can be up to a factor of ~ 2 for the extreme limits of the allowed values of "*El*". As different parts of the sky were scanned in general at different solar elongation angles, there are two possible approaches to correct for the zodiacal emission and obtain the galactic emission from the IRAS measurements: (i) To use information of the IRAS telescope aspects relative to the solar system alongwith the flux density measurements and make a detailed model of the ZE as a function of the solar system based coordinates of the IRAS satellite and its telescope boresight. (ii) To use cruder angular bins to make a local correction. Then use the measurements across the galactic plane, for a chosen galactic longitude at a time. Fit a smooth curve through the points a few degrees (say $\sim 5°$) away from and on both sides of the galactic plane. Now the remainder after subtracting this smooth curve from the observations near the galactic plane ($|b| \leqq 5°$) is a measure of the galactic emission from that galactic longitude which is concentrated on the plane. The process can be repeated to cover the entire galactic longitude range.

Whereas the first approach is ideal for getting high angular resolution and precision of the galactic emission, it requires access to additional information than that available in LORASI and a huge amount of data processing. However, our interest in the present study is to obtain only the crude features of the galactic ridge emission (good to a factor $\leqq 2$, angular resolution $\sim 5°$) in the four IRAS bands. Therfore, the second approach has been followed here.

The measurements of LORASI corresponding to all galactic longitudes and to galactic latitudes within $\pm 25°$ have been used. These are binned such that the bin size is 1° in galactic latitude and 10° in galactic longitude. The averaging over the first and the second sky coverages (HCON 1 and HCON 2) have been performed as the third coverage (HCON 3) may need further corrections to its calibration (see Sect. XI. F of ES).

Of the 51 data points (for $b^{II} = -25°$ to $+25°$) for a given galactic longitude zone, the 40 points corresponding to $|b^{II}| \geqq 6°$ have been used to make a least square fit with a linear combination of Legendre Polynomials of degree up to 2 (higher orders will lack physical justification) which form an orthogonal set over the interval $|b^{II}| \leqq 25°$. The fitted function has been used to approximate the wide angle emission ($b^{II} \leqq 5°$) and the galactic ridge emission has been computed. This has been repeated 36 times to cover the complete galactic longitude range for the first three IRAS bands where the wide angle constitutes the ZE. In the 100 μm band, where the cirrus clouds also make a significant contribution to the emission at higher galactic latitudes, the ZE has been estimated by fitting the ZE spectrum between 60 and 100 μm (see Fig. 2 of Hauser et al., 1984) to the 60 μm zodiacal emission.

References

Adams, F.C., Shu, F.H.: 1985, *Astrophys. J.* **296**, 655

Altenhoff, W.J., Downes, D., Pauls, T., Schraml, J.: 1979, *Astron. Astrophys. Suppl.* **35**, 23

Arp, H.C.: 1966, *Astrophys. J. Suppl.* **14**, 1

Beichman, C.A., Jennings, R.E., Emerson, J.P., Baud, B., Harris, S., Rowan-Robinson, M., Aumann, H.H., Gautier, T.N., Gillett, F.C., Habing, H.J., Marsden, P.L., Neugebauer, G., Young, E.: 1984, *Astrophys. J. Letters*, **278**, L 45

Beichman, C.A, Neugebauer, G., Habing, H.J., Clegg, P.E., Chester, T.J.: 1985, IRAS Catalogs and Atlases Explanatory Supplement, JPL D-1855 (ES)

Benson, P.J., Myers, P.C., Wright, E.L.: 1984, *Astrophys. J. Letters*, **279**, L 27

Caux, E., Puget, J.L., Serra, G., Gispert, R., Ryter, C.: 1985, *Astron. Astrophys.* **144**, 37

Caux, E., Serra, G., Gispert, R., Puget, J.L., Ryter, C., Coron, N.: 1984, *Astron. Astrophys.* **137**, 1

Cox, P., Krügel, E., Mezger, P.G.: 1986, *Astron. Astrophys.* **155**, 380

de Muizon, M., Rouan, D.: 1985, *Astron. Astrophys.* **143**, 160

Désert, F.X., Boulanger, F., Léger, A., Puget, J.L., Sellgren, K.: 1986, *Astron. Astrophys.* **159**, 328

Drapatz, S.: 1979, *Astron. Astrophys.* **75**, 26

Drapatz, S., Michel, K.W.: 1977, *Astron. Astrophys.* **56**, 353

Emerson, J.P., Harris, S., Jennings, R.E., Beichman, C.A., Baud, B., Beintema, D.A., Marsden, P.L., Wesselius, P.R.: 1984, *Astrophys. J. Letters*, **278**, L 49

Frogel, J.A., Persson, S.E.: 1974, *Astrophys. J.* **192**, 351

Frogel, J.A., Persson, S.E., Aaronson, M: 1977, *Astrophys. J.* **213**, 723

Gillett, F.C., Kleinmann, D.E., Wright, E.L., Capps, R.W.: *Astrophys. J. Letters*, **198**, L 65

Harris, S.: 1985, Proc. ESO-IRAM-ONSALA Workshop *Submillimeter Astronomy*, eds. P. Shaver, K. Kjar, p. 527

Hauser, M.G., Gillett, F.C., Low, F.J., Gautier, T.N., Beichman, C.A., Neugebauer, G., Aumann, H.H., Baud, B., Boggess, N., Emerson, J.P., Houck, J.R., Soifer, B.T., WAlker, R.G.: 1984, *Astrophys. J. Letters*, **278**, L 15

Hayakawa, S., Matsumoto, T., Murakami, H., Uyama, K., Thomas, J.A., Yamagami, T.: 1981, *Astron. Astrophys.* **100**, 116

Haynes, R.F., Caswell, J.L., Simons, L.W.J.: 1979, *Australian J. Phys. Astrophys. Suppl.* **48**, 1

Herman, J., Habing, H.J.: 1985, *J.: 1985, Phys. Rep.* **124**, 255

Impey, C.D., Wynn-Williams, C.G., Becklin, E.E.: 1986, *Astrophys. J.* (in press)

Jaffe, D.T., Stier, M.T., Fazio, G.G.: 1982, *Astrophys. J.* **252**, 601

Joseph, R.D., Meikle, W.P.S., Robertson, N.A., Wright, G.S.: 1984, *Monthly Notices Roy. Astron. Soc.* **209**, 111

Keene, J., Harper, D.A., Hildebrand, R.H., Whitcomb, S.E.: 1980, *Astrophys. J. Letters* **240**, L 43

Keene, J., Hildebrand, R.H., Whitcomb, S.E.: 1982, *Astrophys. J. Letters* **252**, L 11

Kronberg, P.P., Biermann, P., Schwab, F.R.: 1985, *Astron. Astrophys.* **291**, 693
Lada, C.J.: 1985, *Ann. Rev. Astron. Astrophys.* **23**, 267
Lauberts, A.: 1982, The ESO/Uppsala Survey of the ESO (B) Atlas
Léger, A., Puget, J.L.: 1984, *Astron. Astrophys.* **137**, L 5
Little, S.J., Price, S.D.: 1985, *Astron. J.* **90**, 1812
Lonsdale, C.J., Persson, S.E., Matthews, K.: 1984, *Astrophys. J.* **287**, 95
Mathis, J.S., Rumpl, W., Nordsieck, K.H.: 1977, *Astrophys. J.* **217**, 425
Mezger, P.G.: 1978, *Astron. Astrophys.* **70**, 565
Mezger, P.G.: 1985, *Birth and Infancy of Stars*, Les Houches Session XLI eds. R. Lucas, A. Omont, R. Stora, p. 31
Neugebauer, G., Habing, H.J., van Duinen, R., Aumann, H.H., Baud, B., Beichman, C.A., Beintema, D.A., Boggess, N., Clegg, P.E., de Jong, T., Emerson, J.P., Gautier, T.N., Gillett, F.C., Harris, S., Hauser, M.G., Houck, J.R., Jennings, R.E., Low, F.J., Marsden, P.L., Miley, G., Olnon, F.M., Pottasch, S.R., Raimond, E., Rowan-Robinson, M., Soifer, B.T., Walker, R.G., Wesselius, P.R., Young, E.: 1984, *Astrophys. J. Letters* **278**, L 1
Olnon, F.M., Baud, B., Habing, H.J., de Jong, T., Harris, S., Pottasch, S.R.: 1984, *Astrophys. J. Letters* **278**, L 41
Pajot, F., Boissé, P., Gispert, R., Lamarre, J.M., Puget, J.L., Serra, G.: 1986, *Astron. Astrophys.* **157**, 393
Price, S.D.: 1981, *Astron. J.*, **86**, 193
Puget, J.L.: 1985, *Birth and Infancy of Stars*, Les Houches Session XLI eds. R. Lucas, A. Omont, R. Stora), p. 77
Puget, J.L., Léger, A., Boulanger, F.: 1985, *Astron. Astrophys.* **142**, L 19
Rieke, G.H., Lebofsky, M.J., Thompson, R.F., Low, F.J., Tokunaga, A.T.: 1980, *Astrophys. J.* **238**, 24
Rowan-Robinson, M., Clegg, P.E., Beichman, C.A., Neugebauer, G., Soifer, B.T., Aumann, H.H., Beintema, D.A., Boggess, N., Emerson, J.P., Gautier, T.N., Gillett, F.C., Hauser, M.G., Houck, J.R., Low, F.J., Walker, R.G.: 1984, *Astrophys. J. Letters* **278**, L 7
Sandage, A.: 1975, *Stars and Stellar Systems*, eds. G.P., Kuiper, Middlehurst, B.M., IX, 1
Soifer, B.T., Rowan-Robinson, M., Houck, J.R., de Jong, T., Neugebauer, G., Aumann, H.H., Beichman, C.A., Boggess, N., Clegg, P.E., Emerson, J.P., Gillett, F.C., Habing, H.J., Hauser, M.G., Low, F.J., Miley, G., Young, E.: 1984, *Astrophys. J. Letters* **278**, L 71
Stier, M.T., Jaffe, D.T., Fazio, G.G., Roberge, W.G., Thum, C., Wilson, T.L.: 1982, *Astrophys. J. Suppl.* **48**, 127
Vorontsov-Velyaminov, B.A., Krasnogorskaja, A.A.: 1962, Morphological Catalogue of Galaxies, Part I, Moscow State University
Vorontsov-Velyaminov, B.A., Arhipova, V.P.: 1964, Morphological Catalogue of Galaxies, Part II, Moscow State University
Vorontsov-Velyaminov, B.A., Arhipova, V.P.: 1963, Morphological Catalogue of Galaxies, Part III, Moscow State University
Vorontsov-Velyaminov, B.A., Arhipova, V.P.: 1968, Morphological Catalogue of Galaxies, Part IV, Moscow State University
Vorontsov-Velyaminov, B.A., Arhipova, V.P.: 1974, Morphological Catalogue of Galaxies, Part V, Moscow State University
Walterbos, R., Schwering, P.: 1985, Annual Report, Sterrewacht Leiden Observatory
Willner, S.P., Soifer, B.T., Russell, R.W., Joyce, R.R., Gillett, F.C.: 1977, *Astrophys. J. Letters* **217**, L 121